Available online at www.sciencedirect.com
ScienceDirect
Earth and Planetary Science Letters 258 (2007) 73–86
EPSL
www.elsevier.com/locate/epsl

Benthic foraminiferal B/Ca ratios reflect deep water carbonate saturation state

Jimin Yu *, Henry Elderfield

The Godwin Laboratory for Palaeoclimate Research, Department of Earth Sciences, University of Cambridge, Downing Street, Cambridge, CB2 3EQ, UK

Received 24 November 2006; received in revised form 13 March 2007; accepted 14 March 2007
Available online 21 March 2007
Editor: M.L. Delaney

Abstract

Boron/calcium ratios were measured in four benthic foraminiferal species (three calcitic: *Cibicidoides wuellerstorfi*, *Cibicidoides mundulus*, and *Uvigerina* spp., and one aragonitic: *Hoeglundina elegans*) from 108 core-top samples located globally. Comparison of coexisting species shows: B/Ca of *C. wuellerstorfi* > *C. mundulus* > *H. elegans* > *Uvigerina* spp., suggestive of strong "vital effects" on benthic foraminiferal B/Ca. A dissolution effect on benthic B/Ca is not observed. Core-top data show large intra-species variations (50–130 μmol/mol) in B/Ca. Within a single species, benthic foraminiferal B/Ca show a simple linear correlation with deep water $\Delta[CO_3^{2-}]$, providing a proxy for past deep water $[CO_3^{2-}]$ reconstructions. Empirical sensitivities of $\Delta[CO_3^{2-}]$ on B/Ca have been established to be 1.14±0.048 and 0.69±0.072 μmol/mol per μmol/kg for *C. wuellerstorfi* and *C. mundulus*, respectively. The uncertainties associated with reconstructing bottom water $\Delta[CO_3^{2-}]$ using B/Ca in *C. wuellerstorfi* and *C. mundulus* are about ±10 μmol/kg. A preliminary application shows that the Last Glacial Maximum (LGM) B/Ca ratios were increased by 12% at 1–2 km and decreased by 12% at 3.5–4.0 km relative to Holocene values in the North Atlantic Ocean. This implies that the LGM $[CO_3^{2-}]$ was higher by ~25–30 μmol/kg at intermediate depths and lower by ~20 μmol/kg in deeper waters, consistent with glacial water mass reorganization in the North Atlantic Ocean inferred from other paleochemical proxies.

Keywords: boron; carbonate ion concentration; benthic foraminifera; proxy

1. Introduction

Measurements on ice cores show that the concentration of carbon dioxide (pCO_2) in the atmosphere was 80–100 ppmv lower during ice ages than it was at pre-industrial times [1]. In order to accurately predict the consequences of man-made CO_2 on future climate it is essential to understand mechanisms causing the change in atmospheric pCO_2 on glacial–interglacial timescales. The ocean is the largest component of the climate system, and marine processes that alter the inventory or distribution of total dissolved inorganic carbon and alkalinity in the oceans are primary potential drivers of atmospheric pCO_2 change on the timescales of glacial/interglacial transitions [2]. Various hypotheses have been suggested to explain the observed atmospheric pCO_2 cycles (e.g., [3–7]), but no consensus has emerged on the specific driver(s) of glacial/interglacial pCO_2 changes. Proxies of oceanic carbonate system parameters are required to provide constraints necessary to evaluate the different mechanisms proposed to

* Corresponding author.
E-mail address: jyu02@esc.cam.ac.uk (J. Yu).

0012-821X/$ - see front matter © 2007 Elsevier B.V. All rights reserved.
doi:10.1016/j.epsl.2007.03.025

account for atmospheric pCO_2 fluctuations. For example, reconstructions of deep water pH and carbonate ion concentrations, [CO_3^{2-}], would provide insights to understand the role of changes in the ratio of organic carbon to $CaCO_3$ in particulate matter exported from the surface to the deep sea [8,9], the effect of vertical nutrient fractionation [4], and the mechanisms of carbonate compensation at glacial/interglacial transitions [3,5,9].

Different approaches have been developed to study changes in past deep ocean [CO_3^{2-}]. In general, available methods can be classified into three categories: carbonate dissolution based proxies, theory based proxies, and empirical relationship based proxies (Table 1). Many studies have been carried out to investigate how deep water pH and [CO_3^{2-}] differed during glacial time [10–17,6], but changes in deep water [CO_3^{2-}] remain uncertain [18]. Conflicting results for deep water [CO_3^{2-}] during the last glacial interval are probably due to limitations and uncertainties in the assumptions underlying different methods (Table 1). For example, carbonate dissolution based proxies are limited to water masses close to the lysocline and suffer the complication that dissolution occurs mainly in sediment pore waters rather than on the sea floor [19,20].

The importance of deep ocean carbonate chemistry warrants the use of additional proxies to resolve conflicts of past deep water [CO_3^{2-}]. In this study, we have developed a novel method to reconstruct deep water [CO_3^{2-}] using boron/calcium ratios in benthic foraminifera. A core top calibration approach was adopted to investigate the feasibility of using B/Ca as a proxy for the deep water CO_2 system. We then compared B/Ca ratios with other geochemical proxies from Holocene and Last Glacial Maximum (LGM) time slices in the North Atlantic Ocean to assess the reliability of this approach for reconstruction of deep water [CO_3^{2-}].

Table 1
Summary of different proxies used for deep water [CO_3^{2-}] reconstructions

Category	Proxy	Changes in deep water [CO_3^{2-}][a]	Complications/limitations	Reference[c]
Dissolution based	$CaCO_3$ MAR[b] and $CaCO_3$ %	Higher in the deep Pacific and lower in the deep Atlantic and the Southern Ocean	Surface water productivity, pore water dissolution	[1–11]
	Foraminiferal shell weight	Consistent with $CaCO_3$ MAR and $CaCO_3$% and further suggest large vertical gradients in [CO_3^{2-}] in the glacial equatorial Atlantic and Pacific	Pore water dissolution, variation in initial weight	[1,4,12–15]
	Normalized shell weight	About 20 μmol/kg lower in the N. Atlantic at ~4 km	Pore water dissolution	[1,4,12,15]
	Foraminiferal assemblage	About 20 μmol/kg decrease at intermediate depth in the western Atlantic and negligible change in other oceans	Surface temperature, pore water dissolution	[1,4,17]
	$\Delta(Mg/Ca)_{planktonic}$	Lower [CO_3^{2-}] at >2.8 km in western tropical Atlantic	Pore water dissolution, initial Mg/Ca ratio	[1,4,18]
Theory based	$\delta^{11}B$	About 100 μmol/kg increase in the whole deep ocean	pK_B^*, species-dependent "vital effects" on $\delta^{11}B$	[19–22]
Empirical relationship based	D_{Zn} and D_{Cd}	About 10–15 μmol/kg lower in the deep N. Atlantic and ~10 μmol/kg lower in the deep tropical Pacific with a ~25–30 μmol/kg peak at Termination I	Seawater [Cd] and [Zn], insensitivity at high $\Delta[CO_3^{2-}]$	[23–25]
	$\Delta(Mg/Ca)_{benthic}$	About 50 μmol/kg higher at 2 km in the N. Atlantic and ~10 μmol/kg higher at 3.3 km in the S. Pacific	Temperature effect on Mg/Ca	[26,27]
	B/Ca	About 25–30 μmol/kg higher at 1–2 km and ~20 μmol/kg lower at 3.5 km in the N. Atlantic		This study

[a]Comparison of the LGM value with the late Holocene; [b]Mass Accumulation Rate; [c]Reference: [1]: Archer [19], [2]: Coxall et al. [13], [3]: Crowley [64], [4]: Emerson and Bender [20], [5]: Farrell and Prell [14], [6]: Farrell and Prell [15], [7]: Howard and Prell [16], [8]: Karlin et al. [66], [9]: Le and Shackleton [67], [10]: Stephens and Kadko [68], [11]: Wu et al. [69], [12]: Barker and Elderfield [62], [13]: Broecker and Clark [12,70], [14]: de Villiers [71], [15]: Lohmann [72], [16]: Barker et al. [11], [17]: Anderson and Archer [10], [18]: Fehrenbacher et al. [63], [19]: Byrne et al. [73], [20]: Kakihana and Kotaka [74], [21]: Pagani et al. [75], [22]: Sanyal et al. [6], [23]: Marchitto et al. [41], [24]: Marchitto et al. [17], [25]: Marchitto et al. [65], [26]: Elderfield et al. [31], [27]: Rosenthal et al. [42].

2. Samples and method

2.1. Samples

We measured B/Ca ratios in three calcitic (*Cibicidoides wuellerstorfi*, *Cibicidoides mundulus* (*kullenbergi*), and *Uvigerina* spp.) and one aragonitic (*Hoeglundina elegans*) benthic species in 108 Holocene sediments from the world's oceans with large data sets for *C. wuellerstorfi* from the Norwegian Sea, the Atlantic, Indian, and Pacific Oceans (Fig. A1 and Table A1). Sediments were verified to be Holocene in age using published benthic and planktonic foraminiferal $\delta^{18}O$ and radiocarbon dates. Several sites from the Indian Ocean only have a few centimeters (~15 cm) of Holocene sediments but omission of these data does not alter the general conclusions of this study.

Down core B/Ca ratios were measured in *C. wuellerstorfi* from BOFS (Biogeochemical Ocean Flux Study) 14K (58.6°N, 19.4°W, 1756 m), 5K (50.7°N, 21.9°W, 3547 m) and 8K (52.5°N, 22.1°W, 4045 m) and in *C. mundulus* from BOFS 17K (58.0°N, 16.5°W, 1150 m). The chronologies of these cores are from Barker et al. [11] and Manighetti et al. [21].

2.2. Analytical methods

For most of core-top samples, approximately 10–15 tests (~250 μg) were hand-picked from the 250–500 μm size fraction and cleaned by the "Cd-cleaning" procedure [22]. The effect of different cleaning methods on B/Ca was tested using large samples. About 0.7 mg of shells (250–500 μm) for each sample were gently crushed and mixed with the aim of homogenizing them as much as possible. The samples were each split into two sub-samples which were respectively subject to the "Mg-cleaning" [23] and "Cd-cleaning" [22] methods. The "Cd-cleaning" procedure includes a reductive cleaning step in order to remove possible oxide coatings cemented onto foraminiferal shells [22]. When larger sample sizes were available, up to 6 sub-samples of foraminiferal shells were crushed separately (not combined after crushing) in order to investigate the natural variability of B/Ca within a single sample. In addition, Rose Bengal dyed and non-stained foraminiferal shells from eight samples were analyzed to detect possible post-mortal influences on B/Ca ratios. Foraminiferal shells from BOFS 17K, 5K and 8K were cleaned by the "Cd-cleaning" procedure [22], while shells from BOFS 14K were cleaned by the "Mg-cleaning" method [23].

B/Ca ratios were analyzed by inductively coupled plasma mass spectrometer (ICP-MS) according to the method described in [24]. On ICP-MS, the B blank is <2% of the consistency standards (B/Ca=150 μmol/mol). When possible, duplicate measurements on the same solution were made for some core-top samples (Table A2). Based on replicate analyses of standards and samples, the precisions are <2.3% (RSD) for B/Ca. $\delta^{13}C$ in *Cibicidoides* genera from BOFS 5K and *C. wuellerstorfi* from BOFS 14K were determined by gas source mass spectrometry. The precision is <0.08‰ (absolute error) for $\delta^{13}C$.

2.3. Hydrographic data

We estimated total dissolved inorganic carbon (DIC), total alkalinity (ALK), together with nutrient levels (PO_4 and SiO_3), salinity (S), bottom water temperature (BWT), and anthropogenic CO_2 from nearby Global Ocean Data Analysis Project (GLODAP) sites [25]. The anthropogenic CO_2 contribution was subtracted from DIC and pre-industrial values including bottom water $[B(OH)_4^-]/[HCO_3^-]$, $[CO_3^{2-}]$, pH (total scale), and the saturation states (Ω) for calcite and aragonite were calculated using CO2sys.xls (Ver. 12) [26] with K_1 and K_2 according to Mehrbach et al. [27] and KSO_4 according to Dickson [28] (Table A1). Assuming constant $[Ca^{2+}]$ in seawater, $[CO_3^{2-}]_{sat}$ is calculated by $[CO_3^{2-}]/\Omega$. The degree of carbonate saturation, $\Delta[CO_3^{2-}]$, is defined as the difference between $[CO_3^{2-}]$ and $[CO_3^{2-}]_{sat}$: $\Delta[CO_3^{2-}]=[CO_3^{2-}]-[CO_3^{2-}]_{sat}$. When calculating $\Delta[CO_3^{2-}]$, $[CO_3^{2-}]_{sat}$ of aragonite was used for *H. elegans* and $[CO_3^{2-}]_{sat}$ of calcite was used for other calcitic species. Seawater total boron concentration was calculated from S by $[B]_{total}$ (μmol/kg)=416*S/35 [29].

3. Core-top results

3.1. Comparability of B/Ca

Core-top B/Ca ratios in four taxa of benthic foraminifera are presented in Table A2. We used both "Mg-cleaning" and "Cd-cleaning" methods to clean 22 *C. wuellerstorfi*, 14 *C. mundulus*, and 3 *Uvigerina* spp. samples (Fig. 1a). Comparison of the two cleaning methods revealed a negligible effect on B/Ca ratios. Measurements of B/Ca for Rose Bengal stained ("recently" live) and unstained (dead) *C. wuellerstorfi* and *C. mundulus* show similar ratios (Fig. 1b), suggesting that benthic B/Ca is not affected by any processes during post-mortal burial and variations of B/Ca reflect a biological precipitation effect. Because of comparable B/Ca ratios for stained and unstained specimens cleaned by different procedures, we have used average B/Ca ratios

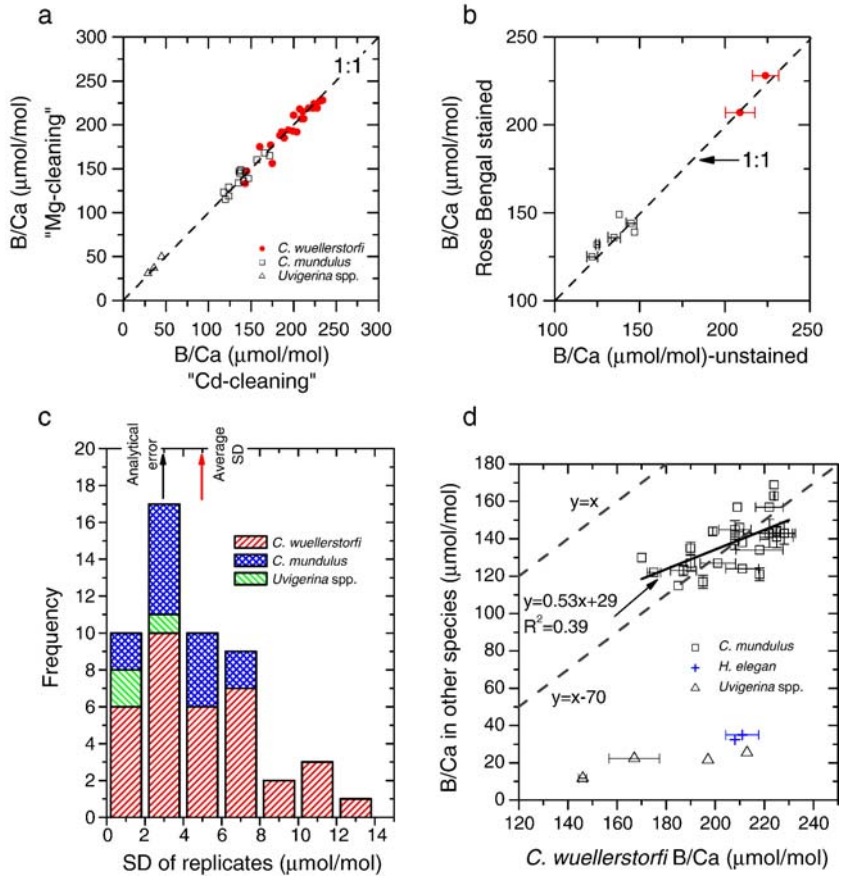

Fig. 1. Comparability and variability of B/Ca data. (a) Effect of different cleaning methods on benthic B/Ca ratios; (b) comparison of B/Ca determined on coexisting unstained and Rose Bengal stained foraminifera; (c) standard deviation (SD) of B/Ca for replicate measurements; (d) comparison of B/Ca in co-existing species. Two 1:1 dashed lines ($y=x$ and $y=x-70$) are shown to assist comparison. The solid line represents the best linear fit for *C. mundulus* vs. *C. wuellerstorfi*.

when replicate measurements were made for the same sample (Table A2).

3.2. Variability of B/Ca

Duplicate measurements of B/Ca allow investigation of natural B/Ca variability within a single sample. Standard deviations (SD) of B/Ca for *C. wuellerstorfi*, *C. mundulus* and *Uvigerina* spp. show a range of 0–14 μmol/mol with an average of ~5 μmol/mol (Fig. 1c). The average SD is larger than the analytical uncertainty of ~3 μmol/mol and hence B/Ca differences between shells from the same sample reflect natural variations of B/Ca within a single sample. The SD depends on the number of duplicate measurements, the amount of shells used for each analysis and the application of homogenization by mixing after crushing. In this study, SD values were calculated based on 2–6 duplicate measurements using 10–15 tests for each analysis (~250 μg) from both separately picked and homogenized samples. Larger variability in B/Ca is expected if smaller sample sizes are used without a homogenization step after crushing.

Measurements of B/Ca for coexisting species within the same sample reveal large inter-species differences (Fig. 1d). *C. mundulus* has B/Ca ratios about 70 μmol/mol lower than *C. wuellerstorfi*, but the differences are not constant and tend to be smaller at lower ratios. In comparison, B/Ca ratios in *Uvigerina* spp. and *H. elegans* are much lower. It is noteworthy that low B/Ca ratios are observed in *H. elegans*, which is aragonitic and expected to be more compatible to host HBO_3^- than calcite [30]. This suggests "vital effects" on the incorporation of boron into benthic foraminiferal carbonates. Vital effects on B/Ca are also observed for planktonic foraminifera [40].

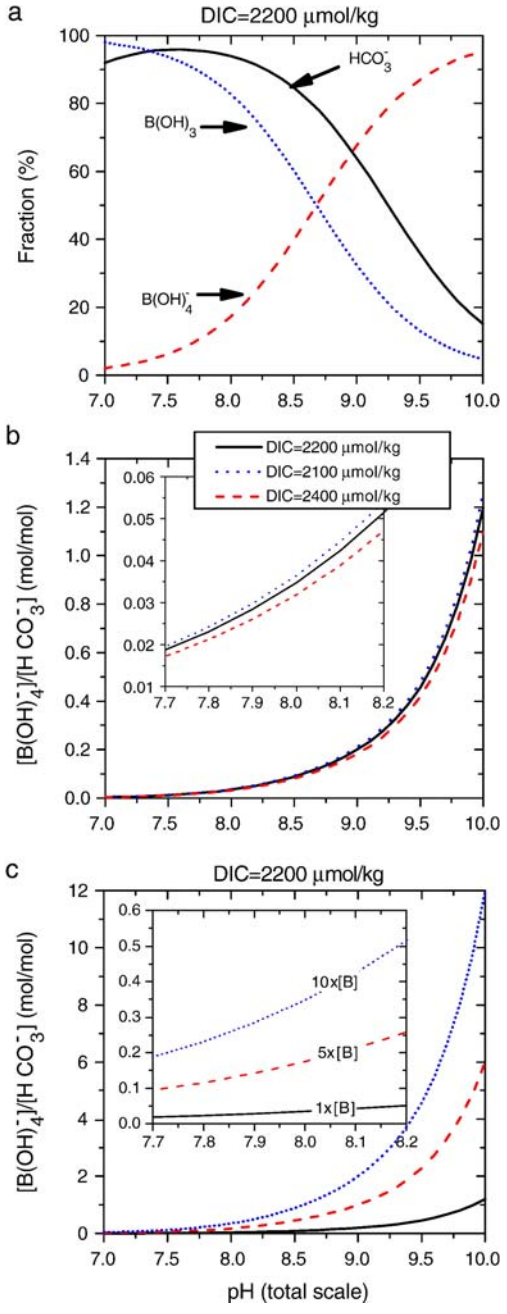

Fig. 2. (a) Fractions of $B(OH)_4^-$, $B(OH)_3$, and HCO_3^- in seawater varying with pH assuming DIC = 2200 µmol/kg and [B] = 416 µmol/kg. (b) Variation of $[B(OH)_4^-]/[HCO_3^-]$ ratios with seawater pH at a constant [B] (416 µmol/kg) and differing DIC. (c) Variation of $[B(OH)_4^-]/[HCO_3^-]$ ratios with seawater pH at a constant DIC (2200 µmol/kg) and differing [B]. This demonstrates possible effects on fluid $[B(OH)_4^-]/[HCO_3^-]$ ratios due to changes in [B] of an internal calcification reservoir associated with foraminiferal carbonates. Insets in (b) and (c) show the pH range observed in the modern deep oceans. All curves are calculated under the conditions of 1 °C and 4 km water depth.

Benthic foraminiferal B/Ca results for core-top samples also display large intra-species variations with B/Ca values of 10–60 µmol/mol in *Uvigerina* spp. and *H. elegans*, 120–170 µmol/mol in *C. mundulus*, and 130–260 µmol/mol in *C. wuellerstorfi* (Table A2). B/Ca ratios in *C. wuellerstorfi* and *C. mundulus* are higher than those in planktonic foraminifera (30–140 µmol/mol) [40,32,6], but lower than those in corals (400–600 µmol/mol) [33–35]. B/Ca ratios in *Uvigerina* spp. and *H. elegans* are similar to those measured in planktonic foraminifera [40,32,6]. Compared with the natural variability of B/Ca of ~5 µmol/mol within a single sample composed of 10–15 specimens (~250 µg), intra-species B/Ca ranges are ~10–25 times larger and suggestive of influences from the calcification environment.

4. Variation of K_D

In seawater, the proportions of the two major boron species, $B(OH)_3$ and $B(OH)_4^-$, vary with pH (Fig. 2a) and $B(OH)_4^-$ is thought to be the primary species

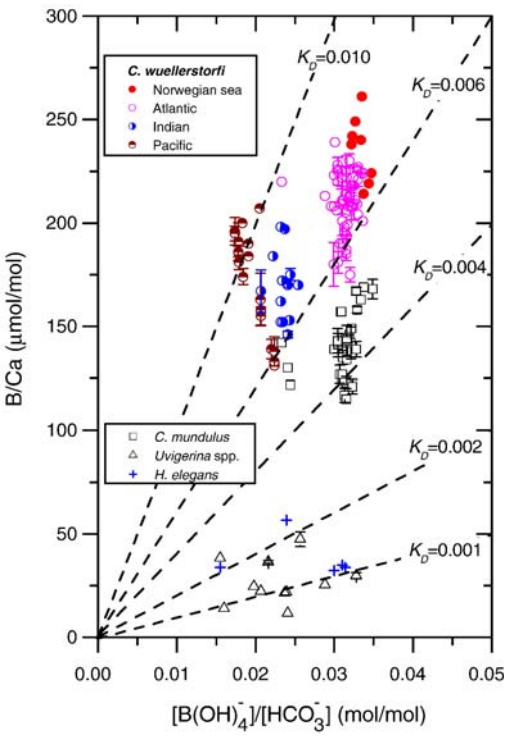

Fig. 3. Seawater $[B(OH)_4^-]/[HCO_3^-]$ vs. B/Ca ratios in four benthic species from the Holocene sediments around global oceans. Dashed lines represent constant K_D values calculated using Eq. (2). Five B/Ca ratios are not included due to possible B contaminations during sample preparation. See Table A2 for details.

incorporated into carbonates [36]:

$$CaCO_3 + B(OH)_4^- \rightarrow Ca(HBO_3) + HCO_3^- + H_2O \quad (1)$$

Because of the existence of HCO_3^- in Eq. (1), B/Ca ratios in $CaCO_3$ would be expected to be influenced by seawater $[HCO_3^-]$ in addition to $[B(OH)_4^-]_{seawater}$. The apparent partition coefficient, K_D, between calcium carbonate and seawater is defined as:

$$K_D = \frac{[HBO_3^{2-}/CO_3^{2-}]_{CaCO_3}}{[B(OH)_4^-/HCO_3^-]_{seawater}} = \frac{[B/Ca]_{CaCO_3}}{[B(OH)_4^-/HCO_3^-]_{seawater}} \quad (2)$$

In Eq. (2), CO_3^{2-} is replaced with Ca^{2+} because their molar ratios are essentially unity in $CaCO_3$. The variation of $[B]_{total}$ of deep seawater is <1% for the studied cores (Table A1) and large fluctuations in $[B]_{total}$ are unexpected on glacial–interglacial timescales due to long residence time of boron in oceans [37–39]. If K_D is constant or can be quantified, the theory summarized above suggests that B/Ca ratios should provide estimates of deep water $[B(OH)_4^-]/[HCO_3^-]$ ratios, which could be used to calculate deep water pH (Fig. 2b and c). This has been found to be the case for planktonic foraminifera for which K_D varies with temperature [40]. None of the species studied plot on a line of constant K_D in Fig. 3, ruling out seawater $[B(OH)_4^-]/[HCO_3^-]$ as the exclusive control on benthic foraminiferal B/Ca. Among the studied species, *C. wuellerstorfi* shows the highest K_D values of 0.005–0.012; *C. mundulus* shows intermediate values of 0.003–0.005; and *Uvigerina* spp. and *H. elegans* show the lowest values of 0.0005–0.003.

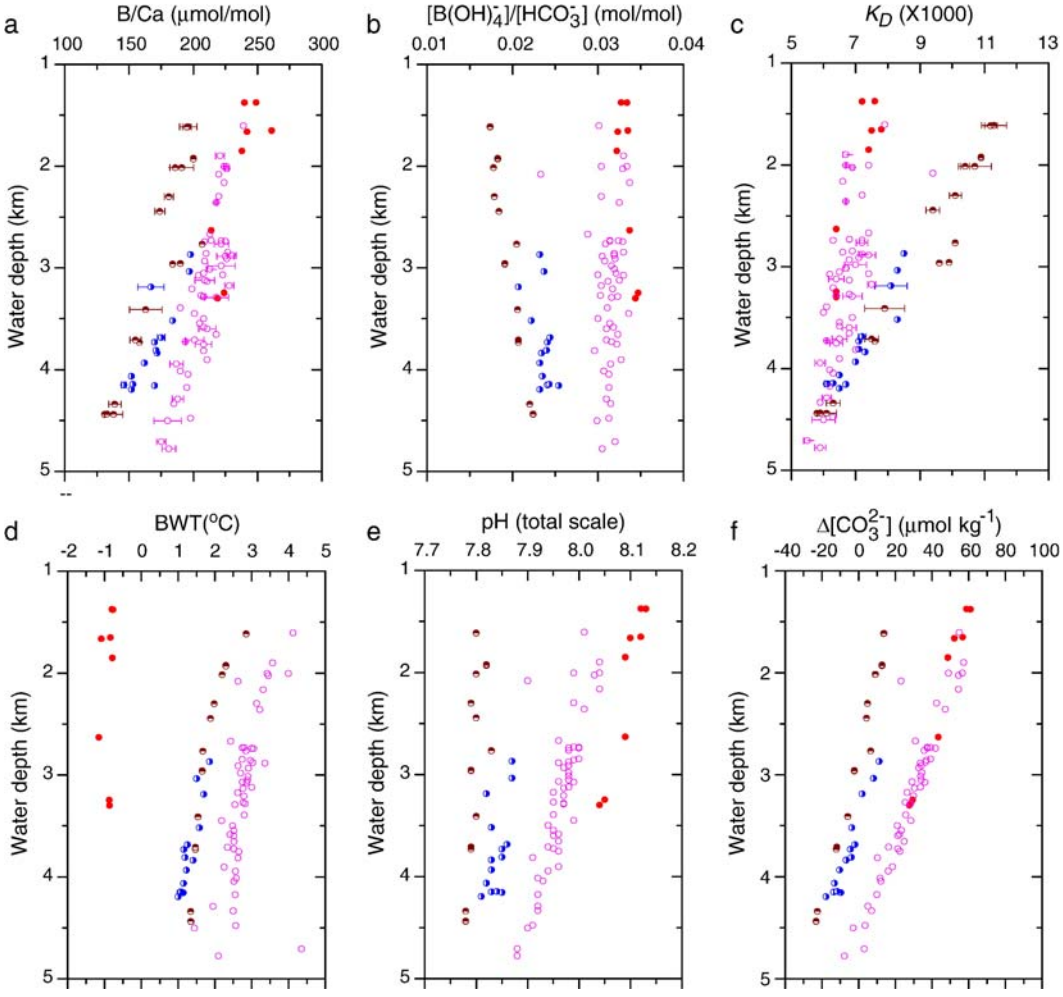

Fig. 4. Distributions vs. water depth of (a) B/Ca in *C. wuellerstorfi*, (b) $[B(OH)_4^-]/[HCO_3^-]$, (c) calculated K_D, (d) BWT, (e) pH, and (f) $\Delta[CO_3^{2-}]$. Symbols as in Fig. 3.

Because the largest global coverage for *C. wuellerstorfi*, we used B/Ca ratios in this species to investigate possible controlling factors on B incorporation by comparing the variation of B/Ca with water depth for samples classified by oceanic regions with the variation of hydrographic properties (Fig. 4). *C. wuellerstorfi* B/Ca decreases almost linearly with water depth in each oceanic region (Fig. 4a). Data from the Norwegian Sea and Atlantic Ocean fall on a similar slope as do data from the Pacific Ocean, although offset by ~40 μmol/mol. The Indian Ocean data, whilst similar to those from the Pacific Ocean, show a steeper gradient in B/Ca. These distribution patterns differ from those of seawater $[B(OH)_4^-]/[HCO_3^-]$ (Fig. 4b). As a consequence, calculated K_D values show very different patterns for samples from different oceans (Fig. 4c). Above 4.3 km, K_D decreases with water depth, samples from the Norwegian Sea and Atlantic Ocean showing lower values than those from the Indo-Pacific Oceans. Below 4.3 km, K_D from different oceans converge, showing a roughly constant value of 0.006. This pattern of distribution of K_D with water depth is distinct from that of BWT (Fig. 4d). BWT is the coldest in the Norwegian Sea, intermediate in the Indo-Pacific Oceans, and the warmest in the Atlantic Ocean. Therefore, no correlation between K_D and BWT is observed (Fig. 5a), unlike the situation for planktonic foraminifera [40]. Unlike benthic D_{Zn} [41], there is no simple correlation between K_D and deep water $\Delta[CO_3^{2-}]$ for core-top samples (Fig. 5b). It proved difficult to quantify K_D using a simple relationship because no significant correlation is observed between K_D and any hydrographic parameter. Core-top B/Ca data indicate that

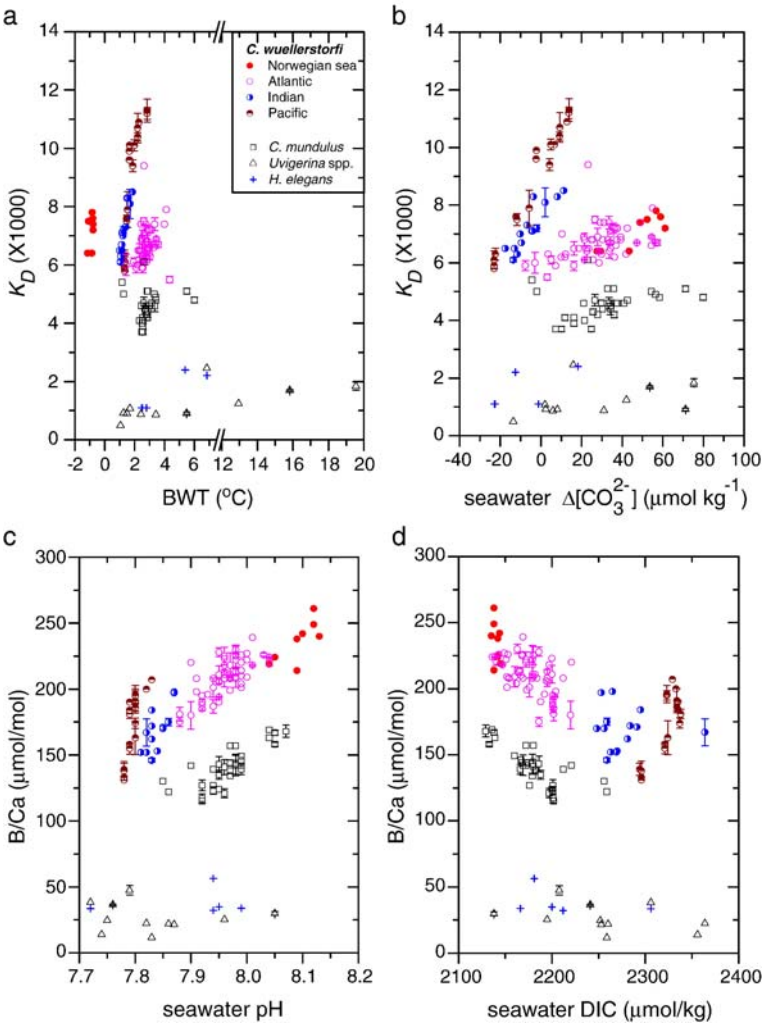

Fig. 5. (a) K_D vs. BWT. (b) K_D vs. seawater $\Delta[CO_3^{2-}]$. (c) B/Ca vs. seawater pH. (d) B/Ca vs. seawater DIC.

B incorporation into benthic foraminifera is different than into planktonic foraminifera [40] and K_D into benthic foraminifera is affected by a combination of factors.

5. An empirical approach

As we were unable to describe the variability in benthic foraminiferal B/Ca through the quantification of K_D, we considered empirical relationships between B/Ca and deep water carbonate system variables. It might be intuitive to link B/Ca with deepwater pH because the proportion to the $[B]_{total}$ of $B(OH)_4^-$, the species though to be incorporated into $CaCO_3$ [36], increases with increasing seawater pH (Fig. 2a). B/Ca ratios of samples from the Norwegian Sea and Atlantic Ocean do decrease with decreasing deep water pH (Figs. 4a, e and 5c). However, this co-variation is not observed in the Indo-Pacific Oceans because B/Ca ratios decrease with increasing water depth whereas bottom water pH remains roughly constant. This indicates only a partial effect of seawater pH on benthic B/Ca. Through changing seawater $[HCO_3^-]$, DIC affects seawater $[B(OH)_4^-]/[HCO_3^-]$ (Fig. 2b) and hence perhaps foraminiferal B/Ca. Fig. 5d suggests that benthic B/Ca is only partially influenced by DIC because *C. wuellerstorfi* B/Ca from the Pacific Ocean increases with DIC, different from the trend defined by samples from other oceans. Therefore, it is also inappropriate to straightly link benthic B/Ca with DIC.

Previous core-top studies have shown that concentrations of a number of trace metals (e.g., Mg [31,42], Zn [41], Cd [17], and Li [43]) in benthic foraminifera decrease with decreasing seawater carbonate saturation state. Fig. 4a and f show a striking similarity in the distribution of B/Ca and $\Delta[CO_3^{2-}]$, both of which decrease linearly with increasing water depth and with lower values in the Indo-Pacific Oceans than the Norwegian Sea and Atlantic Ocean. When B/Ca ratios are plotted against deep water $\Delta[CO_3^{2-}]$, B/Ca ratios in four taxa of benthic foraminifera show significant and coherent correlations with deep water $\Delta[CO_3^{2-}]$. The data can be fitted using simple linear regressions (Fig. 6a and Table 2). The sensitivities of $\Delta[CO_3^{2-}]$ on B/Ca are 1.14±0.048 and 0.69±0.072 μmol/mol per μmol/kg for *C. wuellerstorfi* and *C. mundulus*, respectively. It appears that the sensitivities are sustained at high $\Delta[CO_3^{2-}]$ ranges (Fig. 6a), providing the potential to reconstruct $\Delta[CO_3^{2-}]$ values of waters above the

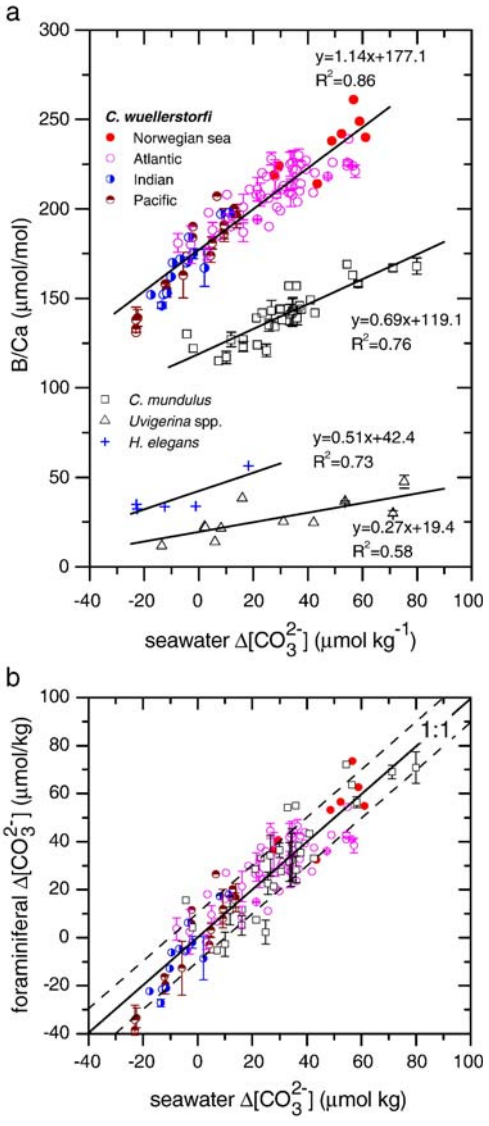

Fig. 6. (a) Bottom water $\Delta[CO_3^{2-}]$ vs. B/Ca ratios in four benthic species from Holocene sediments globally. (b) Foraminiferal $\Delta[CO_3^{2-}]$ calculated from B/Ca using correlations shown in (a) vs. bottom water $\Delta[CO_3^{2-}]$ estimated from the GLODAP dataset [25]. Only values estimated from *C. wuellerstorfi* and *C. mundulus* are shown in (b). Solid lines in (a) represent linear fits for different species. In (b), the 1:1 line (solid) and the ±10 μmol/kg uncertainty envelope (dashed lines) are shown.

Table 2
Correlations between bottom water $\Delta[CO_3^{2-}]$ and B/Ca ratios measured in four benthic species from Holocene sediments

Species	A	B	R^2	*P*-value	*N*[a]
C. wuellerstorfi	1.14±0.048	177.1±1.41	0.86	<0.0001	95(3)
C. mundulus	0.69±0.072	119.1±2.62	0.76	<0.0001	31(1)
Uvigerina spp.	0.27±0.076	19.4±2.99	0.58	0.0063	11
H. elegans	0.51±0.179	42.4±3.12	0.73	0.0653	5(1)

All species are fitted to the form of $B/Ca = A * \Delta[CO_3^{2-}] + B$ using the least square linear regression.
[a]Number in parentheses indicates samples possibly contaminated and not included in the regression analysis.

saturation horizon. Scatters in the regressions may be caused by analytical errors, natural variability in B/Ca, uncertainties in estimating bottom seawater $\Delta[CO_3^{2-}]$, the occasional presence of older foraminifera due to bioturbation and/or lack of latest Holocene sediment. The low R^2 value for *Uvigerina* spp. probably reflects its infaunal habitat, limited measurements, and analyses of B/Ca in mixed species within one genus. We found no other relationship between benthic B/Ca and hydrographic parameters. Based on 1 standard error on the regression, the uncertainties associated with reconstructing bottom water $\Delta[CO_3^{2-}]$ using B/Ca in *C. wuellerstorfi* and *C. mundulus* are about 9.0 and 10.5 μmol/kg, respectively (Fig. 6b). The significant relationship between core-top benthic foraminiferal B/Ca and seawater $\Delta[CO_3^{2-}]$ for species living in various environments in globally distributed geographic areas (pH: 7.7–8.2, temperature: −1–7 °C, and $\Delta[CO_3^{2-}]$: −25–85 μmol/kg) supports the core-top calibrations and provides a robust basis for reconstructing past deep water $\Delta[CO_3^{2-}]$ using benthic B/Ca.

Dissolution effects appear to overprint some metal/Ca ratios proxies from seawater values, which is more prevalent in thinner shelled planktonic foraminifera than the more physically robust benthic species [44,45]. Four lines of evidence argue against a dissolution influence on benthic B/Ca. Firstly, B/Ca ratios are not changed by dissolution in the planktonic foraminifer *Globorotalia inflata* [40]. Secondly, a negligible dissolution effect is suggested by higher K_D values in the Indo-Pacific Oceans (more corrosive) than the Norwegian Sea and Atlantic Ocean (less corrosive) at similar water depth (Figs. 4c and 5b). Thirdly, B/Ca ratios for coexisting unstained and Rose Bengal stained foraminifera show comparable values (Fig. 1b). Because these stained samples are from cores bathed in supersaturated waters (water depth: 2885–4016 m; $\Delta[CO_3^{2-}]$: 11.8–34.5 μmol/kg), the samples have experienced minimal dissolution and therefore the observed correlation between B/Ca and $\Delta[CO_3^{2-}]$ cannot be explained in terms of dissolution. Finally, for all data presented here, a dissolution effect appears unlikely because the B/Ca–$\Delta[CO_3^{2-}]$ slope does not change over the $\Delta[CO_3^{2-}]$ range of −25–85 μmol/kg (Fig. 6a).

6. Incorporation of B into benthic foraminifera

Boron isotope systematics and inorganic precipitation experiments indicate that $B(OH)_4^-$ is the main species incorporated into carbonate [46,47], and B/Ca in $CaCO_3$ is influenced by seawater $[B(OH)_4^-]/[HCO_3^-]$ [36]. In addition, previous studies indicate that changes in the rate of calcite precipitation and crystal growth mechanisms are important controls on B incorporation into $CaCO_3$ [48,46]. The situation becomes more complex with foraminiferal $CaCO_3$ because the formation of biogenic carbonates is heavily mediated by biological processes [49–51]. Vital effects are evident for B incorporation into both planktonic and benthic foraminifera carbonates ([40] and this study).

Because the incorporation of trace elements into foraminiferal $CaCO_3$ is poorly understood [49–51], we can only speculate on some possible mechanisms for the observed relationships between benthic B/Ca and deep water $\Delta[CO_3^{2-}]$ (Fig. 6a). It is suggested that foraminiferal $CaCO_3$ is formed from an internal calcification pool rather than directly from the ambient seawater [49–51]. Due to low K_D ($\ll 1$) and lack of any monotonous correlation between K_D and deep water $\Delta[CO_3^{2-}]$ (Fig. 5b) as observed for benthic D_{Zn} [41], the Rayleigh distillation mechanism proposed by [50] does not apply to benthic B/Ca system. However, the calcification model [50] suggests that chemical compositions of foraminiferal $CaCO_3$ are affected by processes of segregation of seawater into the internal calcification reservoir in addition to seawater chemistry. Although ambient seawater $[B]_{total}$ is roughly constant, $[B]_{total}$ of the direct calcification media may experience large fluctuations due to biological processes during the separation of seawater into the internal calcification pool, which would significantly influence internal fluid $[B(OH)_4^-]/[HCO_3^-]$ and hence carbonate B/Ca ratios (Fig. 4c). Compared with inorganic $CaCO_3$ precipitated in laboratory ($K_D = \sim 0.001$) [47], K_D values into *C. wuellerstorfi* and *C. mundulus* are ~5–10 times higher. This might indicate that $[B]_{total}$ of the internal calcification reservoir of these species is elevated during the process of incorporation of ambient seawater into the internal calcification pool. If the B enrichment factor is proportional to deep water $\Delta[CO_3^{2-}]$ and the variability of internal $[B(OH)_4^-]/[HCO_3^-]$ ratios is largely controlled by changes in the internal $[B]_{total}$, a correlation between benthic B/Ca ratios and ambient seawater $\Delta[CO_3^{2-}]$ would be expected. Of course, any changes in DIC (pH) of the internal reservoir would affect the internal fluid $[B(OH)_4^-]/[HCO_3^-]$ (Fig. 2b) and hence carbonate B/Ca. In these cases, it requires a link between internal DIC (pH) and the ambient seawater $\Delta[CO_3^{2-}]$ in order to explain the observed B/Ca–$\Delta[CO_3^{2-}]$ relationship (Fig. 6a). Previous core-top studies suggest that $\Delta[CO_3^{2-}]$ exerts significant effects on benthic foraminiferal Zn/Ca, Cd/Ca, Mg/Ca, and Li/Ca [31,43,41].

It is noteworthy that boron is incorporated into planktonic foraminifera by a different mechanism and

no carbonate ion effect on B/Ca is observed for planktonic foraminifera [40]. This is not surprising as different incorporation mechanisms into planktonic and benthic foraminifera have been observed for other elements such as Cd and Mg. The partition coefficient of Cd (D_{Cd}) into planktonic foraminifera is largely influenced by the calcification temperature [52], while a temperature influence on benthic D_{Cd} is not observed [53] and D_{Cd} into benthic foraminifera is affected by pressure or carbonate ion saturation [54,17]. In contrast to planktonic Mg/Ca which primarily reflect calcification temperature (e.g., [55–58], a carbonate ion saturation effect is observed in benthic Mg/Ca [31,42]. The reasons are unknown and perhaps are because planktonic and benthic foraminifera respond differently (vital effects?) to seawater carbonate ion variations during the incorporation of trace elements into their shells.

K_D values into benthic foraminifera were calculated using Eq. (2) assuming that $B(OH)_4^-$ is the only species incorporated through the formulation described by Eq. (1) [36]. However, the existence of the HBO_3^{2-} ion is questionable [59]. An attenuated total reflectance Fourier transform infrared (ATR-FTIR) spectroscopic study indicates that both $B(OH)_4^-$ and $B(OH)_3$ are adsorbed onto mineral surfaces and that their relative proportion depends on pH and mineral type [60]. If incorporation of $B(OH)_4^-$ into the $CaCO_3$ lattice is different from that described by Eq. (1) and/or some $B(OH)_3$ is incorporated, it would be inappropriate to use Eq. (2) for calculation of K_D values. The difficulty in quantifying K_D into benthic foraminifera might indicate such uncertainties as well as the strong vital effects associated with biogenic carbonates ([40] and this study). Further studies are required to investigate the mechanisms of incorporation of B into $CaCO_3$.

7. Application to paleoceanography

Due to the long residence time of B in the oceans [37–39], B/Ca–$\Delta[CO_3^{2-}]$ calibrations constructed from global core-top samples should be applicable to estimate deep water $\Delta[CO_3^{2-}]$ for at least the Pleistocene. Deep water $[CO_3^{2-}]$ can be calculated by

$$[CO_3^{2-}] = \Delta[CO_3^{2-}] + [CO_3^{2-}]_{sat} \quad (3)$$

Seawater $[CO_3^{2-}]_{sat}$ is influenced by S, BWT, and pressure (P) and their effects are respectively about 0.5 μmol/kg (3% change in S), 2 μmol/kg (3 °C change in BWT) and 2 μmol/kg (120 m change in P) on glacial–interglacial timescales. Influences from changes in BWT and P are offset and the overall glacial–interglacial effect on $[CO_3^{2-}]_{sat}$ from S, BWT, and P is about 0.5 μmol/kg. Due to the difficulty to estimate past changes in S, BWT and P and because they exhibit insignificant effects on $[CO_3^{2-}]_{sat}$, pre-industrial $[CO_3^{2-}]_{sat}$ values can be used to calculate down core $[CO_3^{2-}]$ through Eq. (3).

We have applied the B/Ca method to reconstruct deep water $[CO_3^{2-}]$ at intermediate and deep water depths in the North Atlantic Ocean for the late Holocene and the LGM (Tables 3a and 3b). At the intermediate depth (Table 3a), *C. mundulus* B/Ca from BOFS 17K (1150 m) show average values of ~167 μmol/mol at late Holocene and ~188 μmol/mol at the LGM, corresponding to a

Table 3a
B/Ca and $\delta^{13}C$ for BOFS 17K and 14K located at intermediate depths from the North Atlantic Ocean

Depth[1]	$\delta^{13}C$[2]	B/Ca	$\Delta[CO_3^{2-}]$	$[CO_3^{2-}]$[3]	Depth[1]	$\delta^{13}C$[2]	B/Ca	$\Delta[CO_3^{2-}]$	$[CO_3^{2-}]$[3]
cm	‰-PDB	μmol/mol	μmol/kg	μmol/kg	cm	‰-PDB	μmol/mol	μmol/kg	μmol/kg
BOFS 17K, 1150 m, *C. mundulus*					BOFS 14K, 1756 m, *C. wuellerstorfi*				
Holocene									
2–3	1.21	166	67	120	2–3	1.12	235	51	110
4–5	1.16	167	68	121	6–7	0.88	239	54	113
6–7	1.21	169	72	124	8–9	1.05	233	49	108
Average	1.19±0.03	167±2	69±2	122±2		1.02±0.12	236±3	51±3	110±3
Modern values[4]			71	124				58	118
LGM									
78–79	1.63	188	99	152	45–46	1.46	274	85	144
80–81	1.40	178	84	137	46–47	1.42	261	73	133
82–83	1.59	197	113	165	48–49	1.51	258	70	130
average	1.54±0.12	188±10	99±14	151±14		1.46±0.05	264±9	76±8	136±8
LGM–Holocene	0.35±0.13	21±10	30±14	30±14		0.45±0.13	29±9	25±8	25±8

[1]Holocene and LGM ages are according to Barker et al. [11] (BOFS 17K) and Manighetti et al. [21] (BOFS 14K); [2]$\delta^{13}C$ are from Bertram et al. [76] and supplemented by this study; [3]seawater $[CO_3^{2-}]$ values were calculated by: $[CO_3^{2-}] = \Delta[CO_3^{2-}] + [CO_3^{2-}]_{sat}$, assuming constant $[CO_3^{2-}]_{sat}$ values of 52.5 μmol/kg and 59.4 μmol/kg for BOFS 17K and 14K, respectively; [4]values are estimated using the GLODAP dataset [25].

Table 3b
B/Ca and $\delta^{13}C$ for BOFS 5K and 8K located at abyssal depths from the North Atlantic Ocean

Depth[1]	$\delta^{13}C$	B/Ca	$\Delta[CO_3^{2-}]$	$[CO_3^{2-}]^3$	Depth[1]	$\delta^{13}C^2$	B/Ca	$\Delta[CO_3^{2-}]$	$[CO_3^{2-}]^3$
cm	‰-PDB	μmol/mol	μmol/kg	μmol/kg	cm	‰-PDB	μmol/mol	μmol/kg	μmol/kg
BOFS 5K, 3547 m, *C. wuellerstorfi*					BOFS 8K, 4045 m, *C. wuellerstorfi*				
Holocene									
6–7	0.71	212	31	115	0–1	0.68	205	25	118
8–9	0.50	202	22	106	2–3	0.68	194	15	108
10–11	0.78	213	24	108	4–5	0.95	196	17	110
Average	0.66±0.14	209±6	25±5	110±5		0.77±0.16	198±6	19±5	112±5
Modern values[4]			23	108				12	105
LGM									
85–86	0.41	186	8	92	101–102	0.32	179	2	95
89–90	0.53	180	3	87	106–107	0.16	182	4	97
90–91	0.31	194	15	100	110–111	0.14	171	−6	87
Average	0.47±0.08	187±7	8±6	93±6		0.21±0.10	177±6	0±5	93±5
LGM–Holocene	−0.19±0.17	−22±9	−17±8	−17±8		−0.56±0.18	−21±8	−19±7	−19±7

[1]Holocene and LGM ages are according to Barker et al. [11]; [2]$\delta^{13}C$ are from Barker et al. [11]; [3]seawater $[CO_3^{2-}]$ values were calculated by: $[CO_3^{2-}]=\Delta[CO_3^{2-}]+[CO_3^{2-}]_{sat}$, assuming constant $[CO_3^{2-}]_{sat}$ values of 84.5 μmol/kg and 92.9 μmol/kg for BOFS 5K and 8K, respectively; [4]values are estimated using the GLODAP dataset [25].

LGM-to-Holocene increase in B/Ca by ~21 μmol/mol (12% change). In BOFS 14K (1756 m), *C. wuellerstorfi* B/Ca at the LGM are higher than at the Holocene by ~29 μmol/mol (12% change). Using the B/Ca–$\Delta[CO_3^{2-}]$ sensitivity of 0.69 μmol/mol per μmol/kg for *C. mundulus* and 1.14 μmol/mol per μmol/kg for *C. wuellerstorfi* (Table 2), the increases in B/Ca translate to a ~25–30 μmol/kg increase in deep water $[CO_3^{2-}]$ (Fig. 7a and Table 3a). *C. mundulus* is thought sometimes to live infaunally at low $\delta^{13}C$ (<1‰) [61]. The reliability of using this species to estimate bottom water $[CO_3^{2-}]$ at BOFS 17K is supported by the fact that (1) $\delta^{13}C$ in this core are always >1‰ (Table 3a), under which condition *C. mundulus* appears unaffected by pore water chemistry [61] and (2) the reconstructed deep water $[CO_3^{2-}]$ at BOFS 17K is consistently higher than in the deeper core BOFS 14K estimated from B/Ca measured in *C. wuellerstorfi*, which is an epifaunal species (Fig. 7a

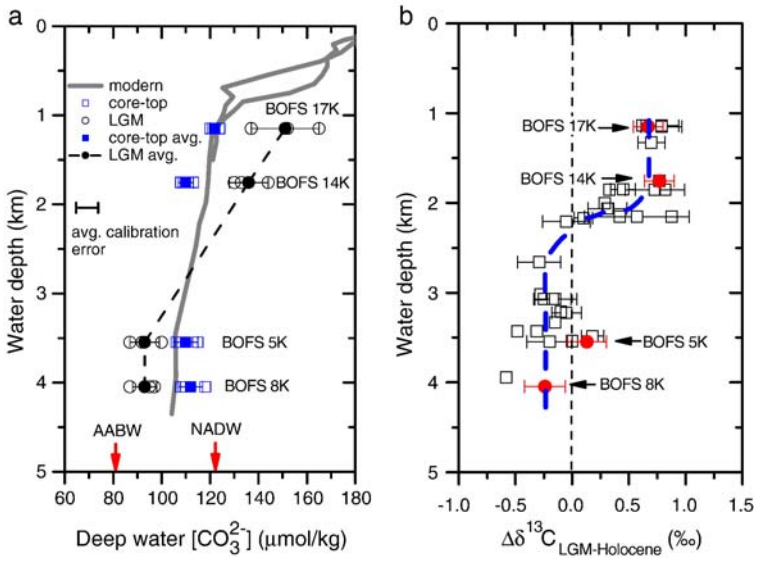

Fig. 7. Depth profiles of (a) deep water $[CO_3^{2-}]$ reconstructed from B/Ca and (b) benthic foraminiferal $\Delta\delta^{13}C$ in the North Atlantic Ocean. In (a), the grey line represents pre-industrial $[CO_3^{2-}]$ for nearby GLODAP sites 22068 (50°N, 20°W) and 27067 (58.9°N, 18.9°W) [25]. Arrows at bottom show modern $[CO_3^{2-}]$ values for AABW and NADW. In (b), $\delta^{13}C$ LGM are corrected by 0.32‰ to account for the global oceanic carbon reservoir change. Additional benthic $\delta^{13}C$ data measured in *Cibicidoides* genera are compiled from literature [54,76–80].

and Table 3a). Compared with intermediate depths, *C. wuellerstorfi* B/Ca from sites BOFS 5K (3547 m) and 8K (4045 m) at the LGM were lower by about 21–22 μmol/mol (12–13% change) relative to Holocene, corresponding to ~17–19 μmol/kg decrease in deep water $[CO_3^{2-}]$ (Fig. 7a and Table 3b) using the B/Ca–$\Delta[CO_3^{2-}]$ sensitivity of 1.14 μmol/mol per μmol/kg for this species (Fig. 6a and Table 2). Such large changes in benthic B/Ca observed in BOFS 17K, 14K, 5K and 8K cannot be explained by changes in $[B]_{total}$ variations (~3%) due to ice volume growth at glacial time. Therefore, B/Ca results suggest that deep water $[CO_3^{2-}]$ at intermediate and deep water depths in the North Atlantic Ocean have experienced contrasting histories since the last glacial time.

The changes in $[CO_3^{2-}]$ observed in BOFS 17K, 14K, 5K and 8K are consistent with evidence from other paleo-chemical proxies. The locations and water depth of BOFS 17K and 14K place them within the Glacial North Atlantic Intermediate Water (GNAIW), which is expected to have higher glacial $[CO_3^{2-}]$ due to lower atmospheric pCO_2 [1] and lower nutrients (Fig. 7b). Foraminiferal shell weight measurements indicate that surface water, which may affect the underlying water masses by mixing and diffusion, had a $[CO_3^{2-}]$ about 50 μmol/kg higher at the LGM than Holocene [62]. Recent benthic Mg/Ca results also suggest a higher $[CO_3^{2-}]$ at ~2 km water depth at the LGM in the North Atlantic Ocean [31]. Water at sites of BOFS 5K and 8K is thought to have been affected by the increased contribution of Antarctic Bottom Water (AABW) at glacial times, which would be expected to lower $[CO_3^{2-}]$ and elevate nutrient contents (Fig. 7). Planktonic foraminiferal Mg/Ca study suggests a lower glacial $[CO_3^{2-}]$ below 2.8 km in the western tropical Atlantic, implying increased influences from glacial AABW during the last glacial time [63]. The glacial reduced carbonate preservation in the deep North Atlantic Ocean indicates a lower $[CO_3^{2-}]$ during glacial time [64]. Benthic Zn/Ca [65] and the normalized shell weight [11] studies suggest that bottom water $[CO_3^{2-}]$ in the North Atlantic was lower by about 10–16 μmol/kg at the LGM than today. Therefore, our B/Ca together with previous studies suggest that deep water $[CO_3^{2-}]$ in the North Atlantic Ocean was strongly affected by water mass reorganization during the last glacial period.

8. Conclusions

Measurements of B/Ca in four benthic species from the global oceans reveal large inter- and intra-species variations (50–130 μmol/mol). Comparison of coexisting species indicates prominent vital effects on benthic foraminiferal B/Ca. No influence of dissolution on benthic B/Ca is observed. Core-top B/Ca results indicate that K_D values into benthic foraminifera are variable but not controlled by temperature. Global benthic B/Ca data show simple linear correlations with deep water $\Delta[CO_3^{2-}]$, providing a quantifiable proxy for deep water $[CO_3^{2-}]$ reconstructions. Preliminary application of the method suggests that deep water $[CO_3^{2-}]$ was elevated by ~25–30 μmol/kg at 1–2 km and lowered by ~20 μmol/kg at 3.5–4.0 km depth during the LGM in the North Atlantic Ocean, consistent with other chemical proxies.

Acknowledgements

We thank Alex Piotrowski, Martin Palmer, and Trond Dokken for very helpful discussion. We are very grateful to Gerald Ganssen for access to foraminifera from the APNAP project. Samples from the NEAPACC project were collected with NERC funding to Nick McCave, Nick Shackleton, and H.E. We thank Heather Johnstone, Johannes Simstich, Frank Bassinot, Babette Hoogeker, and the Ocean Drilling Program (ODP) for core samples, Jason Day and Mervyn Greaves for laboratory assistance, and Linda Booth for help with foraminifera picking. Constructive comments from Editor Peggy Delaney and two anonymous reviewers are appreciated. This research was funded by the Gates Cambridge Trust, European Union 5th Framework Programme project 6C (EVK2-CT-2002-00135), NERC and the Gary Comer Foundation.

Appendix A. Supplementary data

Supplementary data associated with this article can be found, in the online version, at doi:10.1016/j.epsl.2007.03.025.

References

[1] J.R. Petit, J. Jouzel, D. Raynaud, N.I. Barkov, J.M. Barnola, I. Basile, M. Bender, J. Chappellaz, M. Davis, G. Delaygue, M. Delmotte, V.M. Kotlyakov, M. Legrand, V.Y. Lipenkov, C. Lorius, L. Pepin, C. Ritz, E. Saltzman, M. Stievenard, Climate and atmospheric history of the past 420,000 years from the Vostok ice core, Antarctica, Nature 399 (1999) 429–436.

[2] W. Broecker, Glacial to interglacial changes in ocean chemistry, Prog. Oceanogr. 2 (1982) 151–197.

[3] D. Archer, A. Winguth, D. Lea, N. Mahowald, What caused the glacial/interglacial atmospheric pCO_2 cycles? Rev. Geophys. 38 (2000) 159–189.

[4] E.A. Boyle, Vertical oceanic nutrient fractionation and glacial/interglacial CO_2 cycles, Nature 331 (1988) 55–56.

[5] W.S. Broecker, T.H. Peng, The role of $CaCO_3$ compensation in the glacial to interglacial atmospheric CO_2 change, Glob. Biogeochem. Cycles 1 (1987) 15–29.

[6] A. Sanyal, N.G. Hemming, G.N. Hanson, W.S. Broecker, Evidence for a higher pH in the glacial ocean from boron isotopes in foraminifera, Nature 373 (1995) 234–236.
[7] D.M. Sigman, E.A. Boyle, Glacial/interglacial variations in atmospheric carbon dioxide, Nature 407 (2000) 859–869.
[8] D. Archer, E. Maier-Reimer, Effect of deep-sea sedimentary calcite preservation on atmospheric CO_2 concentration, Nature 367 (1994) 260–263.
[9] D.M. Sigman, D.C. McCorkle, W.R. Martin, The calcite lysocline as a constraint on glacial/interglacial low-latitude production changes, Glob. Biogeochem. Cycles 12 (1998) 409–427.
[10] D.M. Anderson, D. Archer, Glacial–interglacial stability of ocean pH inferred from foraminifer dissolution rates, Nature 416 (2002) 70–73.
[11] S. Barker, T. Kiefer, H. Elderfield, Temporal changes in North Atlantic circulation constrained by planktonic foraminiferal shell weights, Paleoceanography 19 (2004), doi: 10.1029/2004PA001004.
[12] W. Broecker, E. Clark, A dramatic Atlantic dissolution event at the onset of the last glaciation, Geochem. Geophys. Geosyst. 2 (2001) (art. no.-2001GC000185).
[13] H.K. Coxall, P.A. Wilson, H. Palike, C.H. Lear, J. Backman, Rapid stepwise onset of Antarctic glaciation and deeper calcite compensation in the Pacific Ocean, Nature 433 (2005) 53–57.
[14] J.W. Farrell, W.L. Prell, Climatic change and $CaCO_3$ preservation: an 800,000 year bathymetric reconstruction from the central equatorial Pacific Ocean, Paleogeography 4 (1989) 447–466.
[15] J.W. Farrell, W.L. Prell, Pacific $CaCO_3$ preservation and $\delta^{18}O$ since 4 Ma: paleoceanic and paleoclimatic implications, Paleoceanography 6 (1991) 485–498.
[16] W.R. Howard, W.L. Prell, Late quaternary $CaCO_3$ production and preservation in the southern-ocean — implications for oceanic and atmospheric carbon cycling, Paleoceanography 9 (1994) 453–482.
[17] T.M. Marchitto, J. Lynch-Stieglitz, S.R. Hemming, Deep Pacific $CaCO_3$ compensation and glacial–interglacial atmospheric CO_2, Earth Planet. Sci. Lett. 231 (2005) 317–336.
[18] H. Elderfield, Climate change: Carbonate mysteries, Science 296 (2002) 1618–1621.
[19] D. Archer, Modeling the calcite lysocline, J. Geophys. Res.—Oceans 96 (1991) 17037–17050.
[20] S. Emerson, M. Bender, Carbon fluxes at the sediment–water interface of the deep-sea — calcium-carbonate preservation, J. Mar. Res. 39 (1981) 139–162.
[21] B. Manighetti, I.N. McCave, M. Maslin, N.J. Shackleton, Chronology for climate change: developing age models for the Biogeochemical Ocean Flux Study cores, Paleoceanography 10 (1995) 513–525.
[22] E. Boyle, L.D. Keigwin, Comparison of Atlantic and Pacific paleochemical records for the Last 215,000 years: changes in deep ocean circulation and chemical inventories, Earth Planet. Sci. Lett. 76 (1985/86) 135–150.
[23] S. Barker, M. Greaves, H. Elderfield, A study of cleaning procedures used for foraminiferal Mg/Ca paleothermometry, Geochem. Geophys. Geosyst. 4 (2003), doi: 10.1029/2003GC000559.
[24] J.M. Yu, J. Day, M. Greaves, H. Elderfield, Determination of multiple element/calcium ratios in foraminiferal calcite by quadrupole ICP-MS, Geochem. Geophys. Geosyst. 6 (2005), doi: 10.1029/2005GC000964.
[25] R.M. Key, A. Kozyr, C.L. Sabine, K. Lee, R. Wanninkhof, J.L. Bullister, R.A. Feely, F.J. Millero, C. Mordy, T.H. Peng, A global ocean carbon climatology: results from Global Data Analysis Project (GLODAP), Glob. Biogeochem. Cycles 18 (2004), doi: 10.1029/2004GB002247.
[26] G. Pelletier, E. Lewis, D. Wallace, A calculator for the CO_2 system in seawater for Microsoft Excel/VBA. Washington State Department of Ecology, Olympia, WA, Brookhaven National Laboratory, Upton, NY, 2005.
[27] C. Mehrbach, C.H. Culberso, J.E. Hawley, R.M. Pytkowic, Measurement of apparent dissociation-constants of carbonic-acid in seawater at atmospheric-pressure, Limnol. Oceanogr. 18 (1973) 897–907.
[28] A.G. Dickson, Thermodynamics of the dissociation of boric-acid in synthetic seawater from 273.15-k to 318.15-k, Deep-Sea Res. Part A, Oceanogr. Res. Pap. 37 (1990) 755–766.
[29] L.R. Uppstrom, Boron/chlorinity ratio of deep-sea water from pacific ocean, Deep-Sea Res. 21 (1974) 161–162.
[30] R.E. Zeebe, D.A. Wolf-Gladrow, CO_2 in Seawater: Equilibrium, Kinetics, Isotopes, Elsevier, Amsterdam, 2001.
[31] H. Elderfield, J.M. Yu, P. Anand, T. Kiefer, B. Nyland, Calibrations for benthic foraminiferal Mg/Ca palaeothermometry and the carbonate ion hypothesis, Earth Planet. Sci. Lett. (2006), doi: 10.1016/j.epsl.2006.07.041.
[32] A. Sanyal, N.G. Hemming, W.S. Broecker, D.W. Lea, H.J. Spero, G.N. Hanson, Oceanic pH control on the boron isotopic composition of foraminifera: evidence from culture experiments, Paleoceanography 11 (1996) 513–517.
[33] S.J. Fallon, M.T. McCulloch, R. Woesik, D.J. Sinclair, Coral at their latitudinal limits: laser ablation trace element systematics in Porites from Shirigai Bay, Japan, Earth Planet. Sci. Lett. 172 (1999) 221–238.
[34] D. Sinclair, Correlated trace element "vital effects" in tropical corals: a new geochemical tool for probing biomineralization, Geochim. Cosmochim. Acta 69 (2005) 3265–3284.
[35] D. Sinclair, L. Kinsley, M. McCulloch, High resolution analysis of trace elements in corals by laser ablation ICP-MS, Geochim. Cosmochim. Acta 212 (1998) 1889–1901.
[36] N.G. Hemming, G.N. Hanson, Boron isotopic composition and concentration in modern marine carbonates, Geochim. Cosmochim. Acta 56 (1992) 537–543.
[37] D. Lemarchand, J. Gaillardet, E. Lewin, C.J. Allegre, The influence of rivers on marine boron isotopes and implications for reconstructing past ocean pH, Nature 408 (2000) 951–954.
[38] D. Lemarchand, J. Gaillardet, E. Lewin, C.J. Allegre, Boron isotope systematics in large rivers: implications for the marine boron budget and paleo-pH reconstruction over the Cenozoic, Chem. Geol. 190 (2002) 123–140.
[39] A.J. Spivack, J.M. Edmond, Boron isotope exchange between seawater and the oceanic-crust, Geochim. Cosmochim. Acta 51 (1987) 1033–1043.
[40] J.M. Yu, H. Elderfield, B. Hönisch, B/Ca in planktonic foraminifera as a proxy for surface water pH, Paleoceanography (2007), doi: 10.1029/2006PA001347.
[41] T.M. Marchitto, W.B. Curry, D.W. Oppo, Zinc concentrations in benthic foraminifera reflect seawater chemistry, Paleoceanography 15 (2000) 299–306.
[42] Y. Rosenthal, C.H. Lear, D.W. Oppo, B.K. Linsley, Temperature and carbonate ion effects on Mg/Ca and Sr/Ca ratios in benthic foraminifera: aragonitic species *Hoeglundina elegans*, Paleoceanography 21 (2006), doi: 10.1029/2005PA001158.
[43] C.H. Lear, Y. Rosenthal, Benthic foraminiferal Li/Ca: Insights into Cenozoic seawater carbonate saturation state, Geology 34 (2006) 985–988, doi: 10.1130/G22792A.1.
[44] S.J. Brown, H. Elderfield, Variations in Mg/Ca and Sr/Ca ratios of planktonic foraminifera caused by postdepositional dissolution: evidence of shallow Mg-dependent dissolution, Paleoceanography 11 (1996) 543–551.

[45] Y. Rosenthal, E.A. Boyle, Factors controlling the fluoride content of planktonic foraminifera — an evaluation of its paleoceanographic applicability, Geochim. Cosmochim. Acta 57 (1993) 335–346.
[46] M.Y. Hobbs, E.J. Reardon, Effect of pH on boron coprecipitation by calcite: further evidence for nonequilibrium partitioning of trace elements, Geochim. Cosmochim. Acta 63 (1999) 1013–1021.
[47] A. Sanyal, M. Nugent, R.J. Reeder, J. Bijma, Seawater pH control on the boron isotopic composition of calcite: evidence from inorganic calcite precipitation experiments, Geochim. Cosmochim. Acta 64 (2000) 1551–1555.
[48] N.G. Hemming, R.J. Reeder, S.R. Hart, Growth-step-selective incorporation of boron on the calcite surface, Geochim. Cosmochim. Acta 62 (1998) 2915–2922.
[49] S. Bentov, J. Erez, Novel observations on biomineralization processes in foraminifera and implications for Mg/Ca ratio in the shells, Geology 33 (2005) 841–844, doi: 10.1130/G21800.1.
[50] H. Elderfield, C.J. Bertram, J. Erez, A biomineralization model for the incorporation of trace elements into foraminiferal calcium carbonate, Earth Planet. Sci. Lett. 142 (1996) 409–423.
[51] J. Erez, The source of ions for biomineralization in foraminifera and their implications for paleoceanographic proxies, Rev. Mineral. Geochem. 54 (2003) 115–149, doi: 10.2113/0540115.
[52] R.E.M. Rickaby, H. Elderfield, Planktonic foraminiferal Cd/Ca: paleonutrients or paleotemperature? Paleoceanography 14 (1999) 293–303.
[53] T.M. Marchitto, Lack of a significant temperature influence on the incorporation of Cd into benthic foraminiferal tests, Geochem. Geophys. Geosyst. 5 (2004), doi: 10.1029/2004GC000753.
[54] E.A. Boyle, Cadmium and $\delta^{13}C$ paleochemical ocean distributions during the stage-2 glacial maximum, Annu. Rev. Earth Planet. Sci. 20 (1992) 245–287.
[55] P. Anand, H. Elderfield, M.H. Conte, Calibration of Mg/Ca thermometry in planktonic foraminifera from a sediment trap time series, Paleoceanography 18 (2003), doi: 10.1029/2002PA000846.
[56] H. Elderfield, G. Ganssen, Past temperature and $\delta^{18}O$ of surface ocean waters inferred from foraminiferal Mg/Ca ratios, Nature 405 (2000) 442–445.
[57] D.W. Lea, D.K. Pak, H.J. Spero, Climate impact of late quaternary equatorial Pacific sea surface temperature variations, Science 289 (2000) 1719–1724.
[58] D. Nüernberg, J. Bijam, C. Hemleben, Assessing the reliability of magnesium in foraminiferal calcite as a proxy for water mass temperatures, Geochim. Cosmochim. Acta 60 (1996) 803–814.
[59] R.H. Byrne, D.R. Kester, Inorganic speciation of boron in seawater, J. Mar. Res. 32 (1974) 119–127.
[60] C. SU, D.L. Suarez, Coordination of adsorbed boron: a FTIR spectroscopic study, Environ. Sci. Technol. 29 (1995) 302–311.
[61] D.A. Hodell, J.H. Curtis, F.J. Sierro, M.E. Raymo, Correlation of late Miocene to early Pliocene sequences between the Mediterranean and North Atlantic, Paleoceanography 16 (2001) 164–178.
[62] S. Barker, H. Elderfield, Foraminiferal calcification response to glacial–interglacial changes in atmospheric CO_2, Science 297 (2002) 833–836.
[63] J. Fehrenbacher, P.A. Martin, G. Eshel, Glacial deep water carbonate chemistry inferred from foraminiferal Mg/Ca: a case study from the western tropical Atlantic, Geochem. Geophys. Geosyst. 7 (2006), doi: 10.1029/2005GC001156.
[64] T.J. Crowley, Calcium-carbonate preservation patterns in the central North-Atlantic during the last 150,000 years, Mar. Geol. 51 (1983) 1–14.
[65] T.M. Marchitto, D.W. Oppo, W.B. Curry, Paired benthic foraminiferal Cd/Ca and Zn/Ca evidence for a greatly increased presence of Southern Ocean Water in the glacial North Atlantic, Paleoceanography 17 (2002), doi: 10.1029/2000PA000598.
[66] R. Karlin, M. Lyle, R. Zahn, Carbonate variations in the Northeast Pacific during the late Quaternary, Paleoceanography 7 (1992) 43–61.
[67] J. Le, N.J. Shackleton, Carbonate dissolution fluctuations in the Western equatorial Pacific during the late Quaternary, Paleoceanography 7 (1992) 21–42.
[68] M.P. Stephens, D.C. Kadko, Glacial–Holocene calcium carbonate dissolution at the central equatorial Pacific seafloor, Paleoceanography 12 (1997) 797–804.
[69] G.P. Wu, M.K. Yasuda, W.H. Berger, Late Pleistocene carbonate stratigraphy on Ontong Java plateau in the western equatorial Pacific, Mar. Geol. 99 (1991) 135–150.
[70] W.S. Broecker, E. Clark, Glacial-to-Holocene redistribution of carbonate ion in the deep sea, Science 294 (2001) 2152–2155.
[71] S. de Villiers, Optimum growth conditions as opposed to calcite saturation as a control on the calcification rate and shell-weight of marine foraminifera, Mar. Biol. 144 (2004) 45–49.
[72] G.P. Lohmann, A model for variation in the chemistry of planktonic-foraminifera due to secondary calcification and selective dissolution, Paleoceanography 10 (1995) 445–457.
[73] R.H. Byrne, W. Yao, K. Klochko, J.A. Tossell, A.J. Kaufman, Experimental evaluation of the isotopic exchange equilibrium $^{10}B(OH)_3 + {}^{11}B(OH)_4^- = {}^{11}B(OH)_3 + {}^{10}B(OH)_4^-$ in aqueous solution, Deep-Sea Res. I 53 (2006) 684–688, doi: 10.1016/j.dsr.2006.01.005.
[74] H. Kakihana, M. Kotaka, Equilibrium constants for boron isotope-exchange reactions, Bull. Res. Lab. Nucl. React. 2 (1977) 1–12.
[75] M. Pagani, D. Lemarchand, A. Spivack, J. Gaillardet, A critical evaluation of the boron isotope-pH proxy: the accuracy of ancient ocean pH estimates, Geochim. Cosmochim. Acta 69 (2005) 953–961.
[76] E.A. Boyle, L. Keigwin, North-Atlantic thermohaline circulation during the past 20,000 years linked to high-latitude surface-temperature, Nature 330 (1987) 35–40.
[77] C.J. Bertram, H. Elderfield, N.J. Shackleton, J.A. Macdonald, Cadmium/calcium and carbon-isotope reconstructions of the glacial Northeast Atlantic-Ocean, Paleoceanography 10 (1995) 563–578.
[78] W.B. Curry, J.-C. Duplessey, L. Labeyrie, N.J. Shackleton, Changes in the distribution of $\delta^{13}C$ of deep water ΣCO_2 between the last glaciation and the Holocene, Paleoceanography 3 (1988) 317–341.
[79] D.W. Oppo, S.J. Lehman, Mid-depth circulation of the subpolar North-Atlantic during the last glacial maximum, Science 259 (1993) 1148–1152.
[80] D.W. Oppo, S.J. Lehman, Suborbital timescale variability of North-Atlantic deep-water during the past 200,000 years, Paleoceanography 10 (1995) 901–910.